QM/MM Study of Catalytic Methyl Transfer by the N^5-Glutamine SAM-Dependent Methyltransferase and Its Inhibition by the Nitrogen Analogue of Coenzyme

RUIBO WU, ZEXING CAO
Department of Chemistry and State Key Laboratory of Physical Chemistry of Solid Surfaces, Xiamen University, Xiamen 361005, China

Received 8 March 2007; Revised 8 May 2007; Accepted 17 May 2007
DOI 10.1002/jcc.20793
Published online 25 June 2007 in Wiley InterScience (www.interscience.wiley.com).

Abstract: The combined density functional quantum mechanical/molecular mechanical (QM/MM) approach has been used to investigate methyl-transfer reactions catalyzed by the N^5-glutamine S-adenosyl-L-methionine (SAM)-dependent methyltransferase (HemK) and the coenzyme-modified HemK with the replacement of SAM by a nitrogen analogue. Calculations reveal that the catalytic methyl transfer by HemK is an energy-favored process with an activation barrier of 15.7 kcal/mol and an exothermicity of 12.0 kcal/mol, while the coenzyme-modified HemK is unable to catalyze the methyl transfer because of a substantial barrier of 20.6 kcal/mol and instability of the product intermediate. The results lend support to the experimental proposal that the nitrogen analogue of the SAM coenzyme should be a practicable inhibitor for the catalytic methyl transfer by HemK. Comparative QM/MM calculations show that the protein environment, especially the residues Asn197 and Pro198 in the active site, plays a pivotal role in stabilizing the transition state and regulating the positioning of reactive groups.

 J Comput Chem 29: 350–357, 2008

Key words: QM/MM calculations; methyltransferase; methylation; inhibition

Introduction

Catalytic methyl transfer reactions by a family of methyltransferases are involved in numerous cellular processes including DNA replication, RNA transport, protein repair, and chromatin regulation.[1–6] Methylation of amino acid residues can function as a reversible signal and it plays an important role in the termination of protein translation.[7]

The methyl transfer from the coenzyme S-adenosyl-L-methionine (SAM) sulfur to the glutamine nitrogen is executed by the N^5-glutamine SAM-dependent methyltransferase (HemK),[8,9] where the SAM coenzyme behaves as the methyl donor and the glutamine substrate behaves as the methyl acceptor as shown in Scheme 1. HemK catalyzes the methyl-transfer reaction by converting SAM and N^5-glutamine (NGLN) into corresponding S-adensoyl-L-homocysteine (SAH) and methyl-glutamine (MGLN), which is the key step for the enzymatic reaction. In the suggested catalytic mechanism, the positioning of NGLN and MGLN with respect to the NPPY motif was regulated by two hydrogen bonds to residues Asn197 and Pro198.[10]

The Hemk gene was initially found in *Escherichia coli*,[11] and its crystal structure reveals two structural domains: a five helix bundle substrate binding domain at the N terminus, and a catalytic domain at the C terminus. On the basis of sequence analysis of HemK, it was assumed that HemK was itself an SAM-dependent DNA methyltransferase.[12] However, subsequent experimental studies found that HemK was not directly involved in the heme biosynthetic route and it was unable to methylate DNA.[7,13]

The crystal structures of HemK provide clear yet static pictures of the active site. On the basis of the three-dimensional spatial arrangement of atoms, both Asn197 and Pro198 have been identified as two key residues in the methyl-transfer process.[10] However, mechanistic details, relative energies of reactive species, effects of protein environments, and solvent molecules on this biochemical process are still unclear. Understanding of the biochemical process at the atomic scale requires further theoretical calculations.

A reliable description of a chemical reaction generally requires sophisticated quantum mechanics (QM) methods. At

Correspondence to: Z. Cao; e-mail: zxcao@xmu.edu.cn

Contract/grant sponsor: National Science Foundation of China; contract/grant numbers: 20673087, 20473062, 20423002, 20233020

Contract/grant sponsor: Ministry of Science and Technology; contract grant number: 2004CB719902

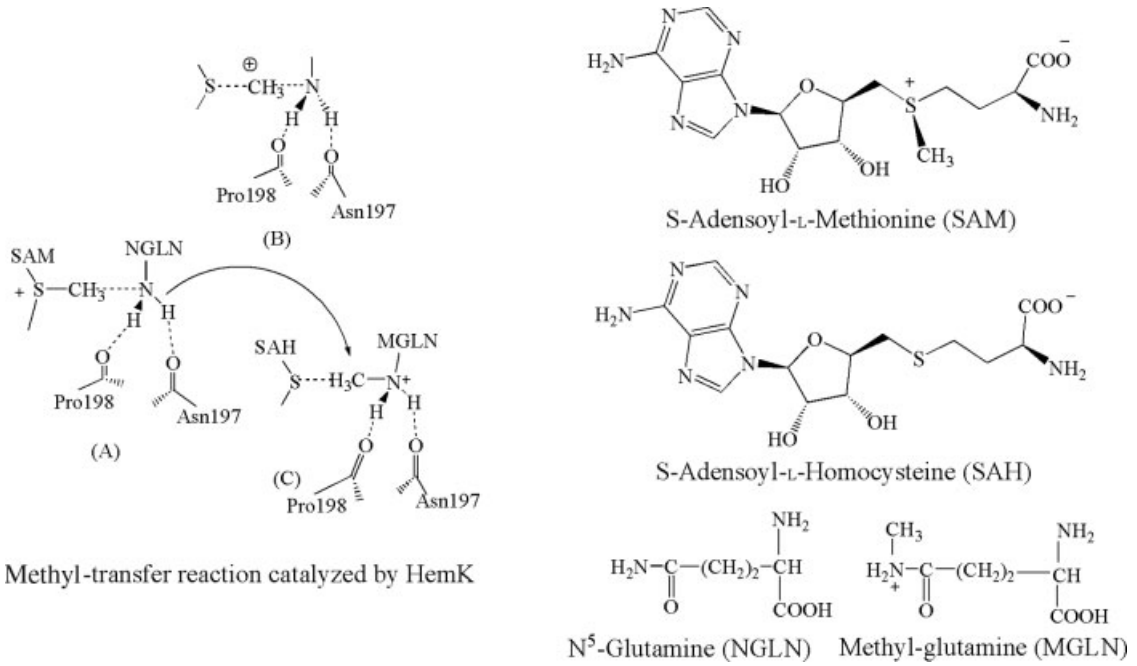

Scheme 1.

present, the full QM treatment on large biomolecules is still impractical. Fortunately, the combined quantum mechanics and molecular mechanics (QM/MM) approach can circumvent this dilemma between the computational cost and accuracy by partitioning the target system into a QM region and a MM region.[14–18] Within the QM/MM model, the QM region only comprises a few atoms directly involved in the chemical reaction, and the MM region is composed of remaining atoms. More recently, the QM/MM methodology has succeeded in description of the methyl transfer reaction catalyzed by the catechol *O*-methyltransferase (COMT), the histone lysine methyltransferase (SET7/9), and the glycine *N*-methyltransferase (GNMT).[19–24]

In the present study, we have performed QM/MM calculation to explore the methyl transfer catalyzed by HemK in condensed phase. We extended our computational study to the coenzyme-modified Hemk, where SAM was replaced by its nitrogen analogue (MAAM) as shown in Scheme 2. The nitrogen analogue has been synthesized and it was assumed to be an effective inhibitor in the enzymatic reaction of methyl transfer.[25,26]

Methods

The complete computational model was built by solvating the crystal structure of HemK (PDB code: 1NV8) in a water sphere of 30 Å radius, followed by 45 ps molecular dynamics (MD) simulations with CHARMM[27] at the MM level to bring the system to an equilibrium state as shown in Figure 1. This spherical model contains 12,787 atoms, including the HemK protein and 2791 water molecules. The equilibrated configuration was used in the subsequent ONIOM and QM/MM calculations. In the geometry optimization and frequency calculation by the ONIOM approach, only 26 atoms from residues MEQ400(NGLN), SAM300(SAM), Asn197, and Pro198 in the active site were explicitly treated by the B3LYP functional, and the overall DFT-AM1 two-layer

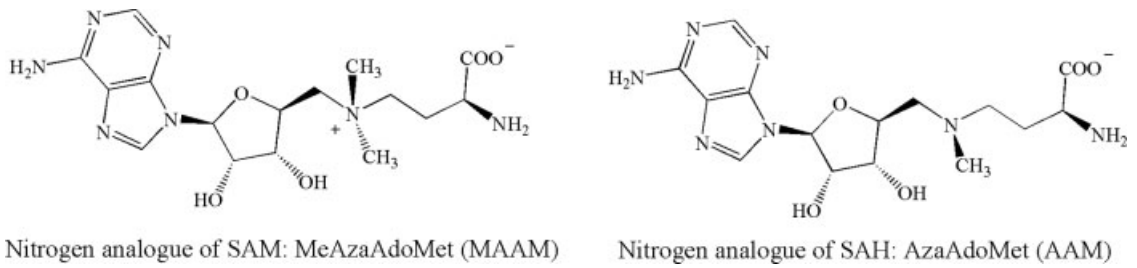

Scheme 2.

ONIOM system consists of 102 atoms. The B3LYP functional[28] and the 6-31G(d) basis set implemented in the Gaussian03 package[29] have been used in the ONIOM calculation.

In the QM/MM geometry optimization of the HemK system, the QM/MM region comprises 120 QM atoms (defined by including selected NGLN/MGLN, SAM/SAH, residues Asn197 and Pro198, and seven waters, see Fig. 1) and 2169 MM atoms (defined by including all residues within 15 Å around the sulfur atom of SAM). Similarly, in the subsequent QM/MM treatment of the coenzyme-modified HemK with replacement of SAM by MAAM, the QM region in the MAAM reaction system was composed 124 atoms, and the MM region was defined by including all residues within 15 Å around the nitrogen atom substituting for sulfur in MAAM.

The RMS deviation of the optimized HemK protein with reference to the crystal structure is 0.88 Å, and thus the QM/MM geometry optimization shows good agreement with the experimental structure. For example, the optimized (SAM)—S—CH_3.....NH_2—(NGLN) distances (refer to Figure 3a) are 1.835 and 3.250 Å, respectively, which are comparable to corresponding experimental values of 1.834 and 3.326 Å.[10]

The B3LYP functional and the 6-31G(d) basis set were used for the QM part in the QM/MM calculation, and the MM part was described by the CHARMM22 force field.[30] An electronic embedding scheme[31a] incorporating the MM charges into the one-electron Hamiltonian of the QM treatment and hydrogen link atoms with charge shift model[31b,c] for the QM/MM boundary were adopted in the QM/MM treatment. The QM/MM calculations were performed with the ChemShell package[32] integrating TURBOMOLE[33] and DL-PLOY[34] programs. The default convergence criteria have been employed in the QM/MM geometry optimization with the HDLC optimizer[35] for reactant and product. In the transition state search, an elaborated initial structure from the potential energy surface scan has been adopted, and a reaction core of three atoms directly involved in the methyl transfer was chosen. Specifically, the L-BFGS steps were executed for all atoms of the active region except the reaction core until the environment convergence was accomplished followed by one partitioned rational function optimizer (P-RFO) step for the reaction core using an explicit Hessian. This process was iterated until the largest gradient component in the core was less than 1.35×10^{-3} E_h a_0^{-1}.

Results and Discussion

Catalytic Methyl Transfer by HemK

The methyl-transfer reaction induced by HemK was explored by both ONIOM and QM/MM approaches. The ONIOM- and QM/MM-optimized structures of reactant (R), transition state (TS), and product (P) are shown in Figures 2 and 3, respectively. Corresponding relative energies in the methyl-transfer reaction are shown in Figure 4. The nature of species has been assessed by frequency calculations at the ONIOM level. Mulliken charge populations of selected atoms and groups of the active site at different reaction states of HemK are presented in Table 1.

Equilibrium Geometries

As Figures 2 and 3 show, the methyl-transfer reaction is a typical S_N2 nucleophilic substitution reaction, like other methyltransferases.[20,23,24] For the initial state, the QM/MM calculations predicted that the distance between the methyl carbon and the N atom in NGLN is 3.250 Å (3.477 Å by ONIOM), and the bond angle of (SAM)—S—CH_3···N(—NGLN) is 175.0° (150.3° by ONIOM). The hydrogen bond distances of (NGLN—)NH···OC(—Pro198) and (NGLN—)NH···OC (—Asn197) are 1.884 and 2.361 Å (2.032 and 2.387 Å by ONIOM), respectively. The (SAM—)S···CH_3 separation increases from 1.835 (R) to 2.401 Å (TS), and to 3.957 Å (P) as the methyl-transfer reaction progresses (Fig. 3). During the reaction process, the positioning of —NH_2 in NGLN towards the coming methyl was maintained by the hydrogen bond interactions, which may facilitate the methyl accommodation by NGLN.

ONIOM- and QM/MM-optimized geometries in Figures 2 and 3 show quite different angles of S···CH_3···N in the active site for all states of HemK. Generally, the QM/MM calculations predict nearly linear S···CH_3···N arrangement in reaction, while such geometrical feature only appears in the transition state at the ONIOM level. This difference in optimized geometries can be ascribed into the confining effect of protein environments.

Relative Energetics

ONIOM and QM/MM relative energy profiles have been presented in Figure 4. As Figure 4 displays, ONIOM calculations indicate that the reaction proceeds to the transition state with a barrier of 18.8 kcal/mol, and the overall reaction is exothermic by 8.6 kcal/mol. The transition state of HemK has one imaginary frequency of -410 cm^{-1} and the imaginary mode corresponds to an in-line S_N2 reaction coordinate. ONIOM-predicted free energies of reaction ΔG and reaction barrier are -8.0 and 19.5 kcal/mol, respectively. At the QM/MM level, the barrier was reduced to 15.7 kcal/mol and the exothermicity was increased to 12 kcal/mol, showing remarkable effect of the protein environment on the methyl-transfer reaction.

As Table 1 shows, this methyl transfer actually is a migration process of methyl cation. As the reaction progresses to the transition state, the —CH_3 group has a charge population of $+0.35$ by QM/MM ($+0.49$ by ONIOM). Notice that the electronegative oxygen atoms in the nearby residues Ala218 and Asn197 are at 2.25 and 2.21Å away from the methyl (Fig. 3) and their electrostatic interactions will stabilize the transition state and reduce the barrier as shown by QM/MM calculations. The ONIOM calculations on truncated models of the active site at different reaction states indicate the presence of Ala218 approximately reduce the barrier by about 1 kcal/mol relative to the reactant state. In comparison with the reactant state, the hydrogen bond interactions between MGLN and Asn197 and Pro198 at the product state become stronger as shown in Figure 3. Such hydrogen bond adjustment results in the reaction more favored thermodynamically.

To evaluate the role of residues Asn197 and Pro198, a simplified active site model without involvement of Asn197 and Pro198 has been considered in the ONIOM calculation. As Figure 4 shows, the methyl-transfer reaction has a substantial

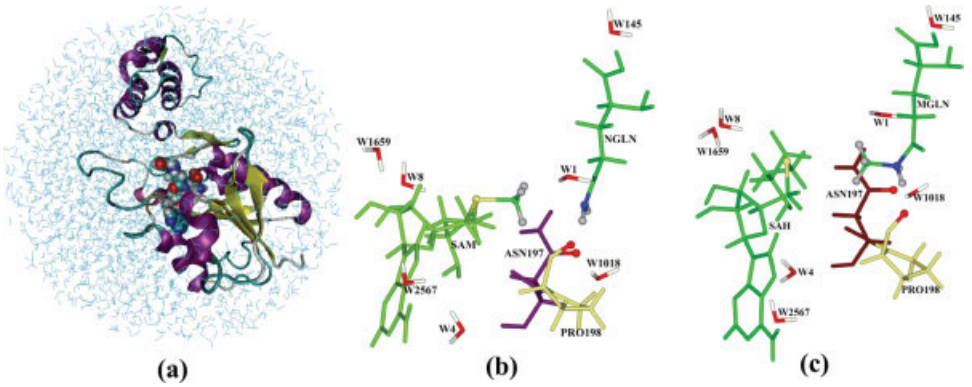

Figure 1. (a) The final solvated model of HemK, where the CPK structure highlights the active site. (b) The active site structure of HemK at its initial state. (c) The active site structure of HemK at its product state. [Color figure can be viewed in the online issue, which is available at www.interscience.wiley.com.]

barrier of 34.6 kcal/mol, and it is endothermic by 9.3 kcal/mol without presence of residues Asn197 and Pro198. These results confirm that the residues Asn197 and Pro198 play an important role in methylation as suggested experimentally.[10]

Orientation and Confining Effects

Although the transition-state stabilization was considered as a key factor responsible for the catalytic activity of enzymes, biochemical observations argued against that the stabilization

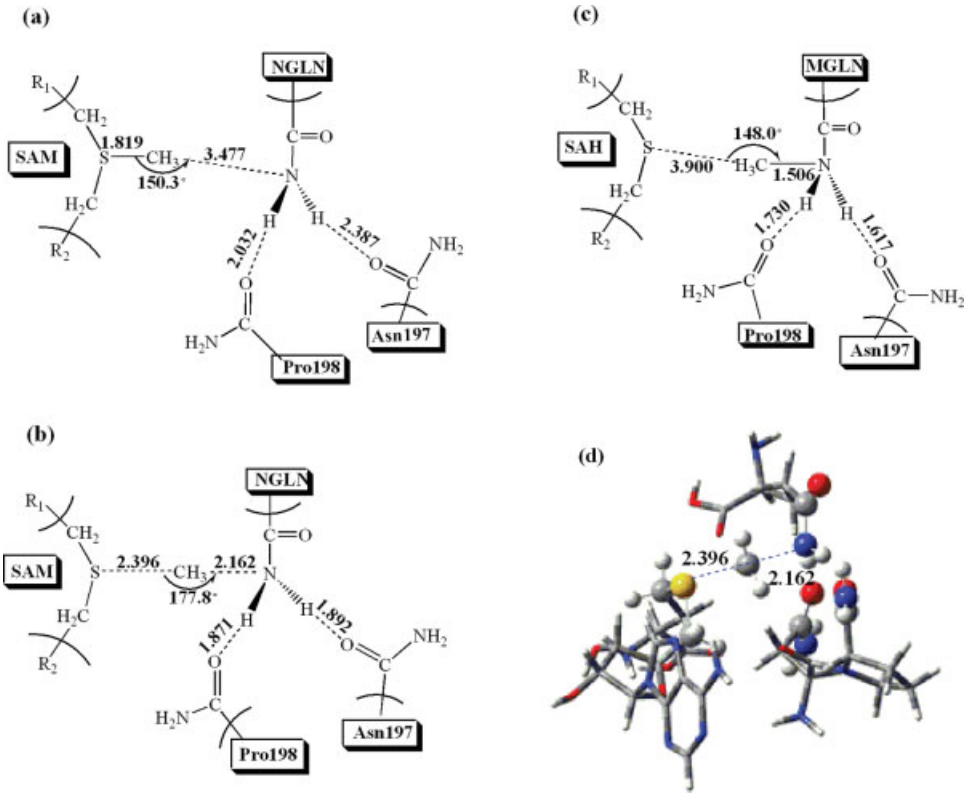

Figure 2. ONIOM-optimized structures of reactant (a), transition state (b and d), and product (c) in the methyl transfer reaction (The ball and stick structure for B3LYP atoms; the tube structure for AM1 atoms). [Color figure can be viewed in the online issue, which is available at www.interscience.wiley.com.]

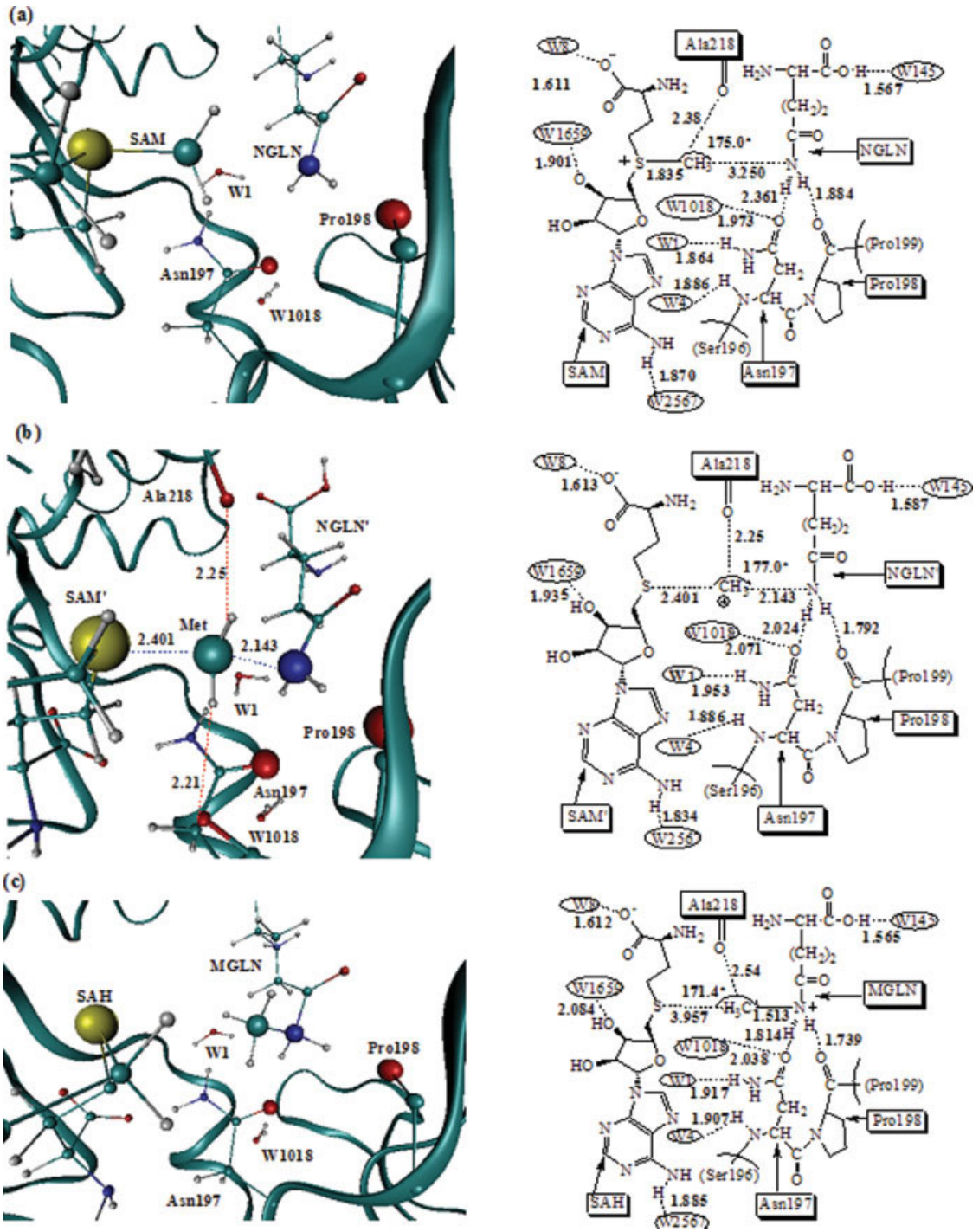

Figure 3. QM/MM-optimized structures of reactant (a), transition state (b), and product (c) in the methyl transfer reaction of HemK (QM = B3LYP; MM = CHARMM; "W" indicates water). [Color figure can be viewed in the online issue, which is available at www.interscience.wiley.com.]

is not yet sufficient for enzymatic catalytic efficiency.[36] Recent theoretical studies also reveal that the predicted barrier strongly depends on the nucleophilic attack distance and angle of the reactant conformation in the methyl-transfer reaction catalyzed by the histone lysine SAM-dependent methyltransferase.[23]

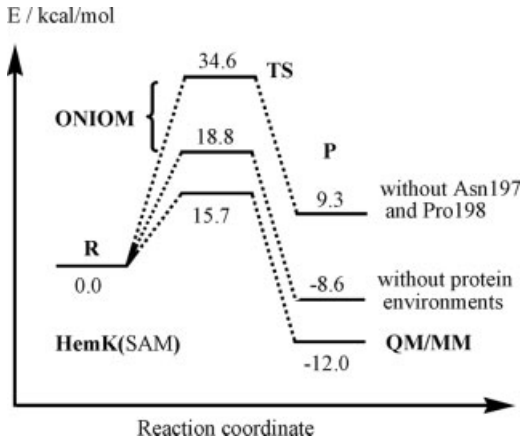

Figure 4. ONIOM and QM/MM relative energy profiles along the methyl-transfer reaction pathway in the simplified active site model and in HemK (QM = B3LYP; MM = CHARMM).

Present MD simulation and QM/MM calculation yield the reactant conformation as shown in Figure 3a, where the SAM coenzyme and the substrate NGLN are nicely confined in the reaction region. The protein environment and the hydrogen bond network around the active site maintain a nearly linear S···C···N conformation for the S_N2 reaction, where the lone pair of the nitrogen atom in NGLN is directed toward the methyl carbon. Such spatial orientation and confining from the protein skelecton and hydrogen bond interactions make the methyl transfer become facile.

Catalytic Methyl Transfer by the Coenzyme-Modified HemK

The nitrogen analogue of SAM (MAAM, see Scheme 2) was suggested to be an inhibitor for the methyl transfer. To have insight into the plausible inhibitive role of the coenzyme analogue, the methyl-transfer reaction catalyzed by the coenzyme-modified HemK has been studied by the QM/MM calculation. The optimized structures of reactant, transition state, and product are shown in Figure 5. The relative energies for the methyl-transfer reaction are depicted in Figure 6. Mulliken charge populations are incorporated into Table 1.

Previous experiments pointed out that this coenzyme analogue could be bound to the *Escherichia coli* methionine repressor protein more tightly than the coenzyme SAM itself.[25] The coenzyme analogue thus was expected to be an effective inhibitor of the SAM-dependent methyl-transfer enzymatic reaction. Our MD simulation and QM/MM geometry optimization indeed bring an initial reactant conformation of the coenzyme-modified HemK to an equilibrated structure as shown in Figure 5, which is quite similar with the equilibrated reactant state of HemK.

The reactant and transition states of the coenzyme-modified HemK have a nearly linear N···C···N conformation in the active site, like HemK. In the product state, the N···C—N angle is 159.6°, smaller than the corresponding angle of 171.4° in HemK. As Figure 6 displays, the activation energy for the catalytic methyl transfer by the modified HemK is 20.6 kcal/mol, which is remarkably higher than the barrier of 15.7 kcal/mol in Figure 4. Furthermore, the overall process is endothermic by 5.2 kcal/mol, and thus it unlikely occurs in practice. The large barrier and instability of the intermediate product may make the nitrogen analogue of SAM serve as a practicable inhibitor to the methyl-transfer reaction as assumed experimentally.

To elucidate such thermodynamic differences in the methyl-transfer reactions catalyzed by HemK and the coenzyme-modified HemK enzymes, we examined chemical bond and bonding changes as the reactions progress. For HemK, the methyl transfer from SAM to NGLN will break relatively weaker S—C bond and make strong N—C bond. The formation of strong C—N bond at the product state as well as the strengthening of H-bond interactions around the substrate is responsible for the thermodynamic favorableness in the methyl transfer. For the coenzyme-modified HemK, only the C—N bond breaking and making was involved in the methyl-transfer process. As Figure 5 displays, the C—N bond length is almost unchanged at the reactant and product states. Why the reaction is endothermic by 5.2 kcal/mol? To understand such notable endothermicity, primary calculations on simplified models of $(CH_3)_4N^+$ and $(HCO)(CH_3)NH_2^+$, served as the nitrogen structural environments in the coenzyme MAAM and the substrate MGLN respectively, have been performed. B3LYP calculations show that the N—CH_3 bond scission requires 85.8 kcal/mol for $(HCO)(CH_3)NH_2^+$ and 125.3 kcal/mol for $(CH_3)_4N^+$ respectively, showing that the bond dissociation behavior can be significantly modified by its structural environment. Molecular orbital (MO) analyses reveal that the highest-occupied MO has a delocalized bonding feature around the tetrahedral nitrogen in $(CH_3)_4N^+$, which may stabilize the positively charged region. In $(HCO)(CH_3)NH_2^+$, the presence of hydrogen atoms linked to nitrogen makes the delocalization impossible. Furthermore, the Milliken charge populations indicate that the N—CH_3 bond can be strengthened by partial ionic bonding interactions in $(CH_3)_4N^+$. A thorough understanding of such striking energetics effect of local structural surrounding change on the bond scission requires further theoretical investigation.

Table 1. Mulliken Charge Populations of Selected Atoms and Groups in the Active Sites of HemK and the Coenzyme-Modified HemK at Their Different Reaction States by QM/MM and ONIOM.

State	S	—CH_3	—NH_2
HemK (SAM)			
R	0.54 (0.83)[a]	0.11 (0.07)	−0.07 (0.06)
TS	0.22 (0.14)	0.35 (0.49)	−0.01 (0.10)
P	0.07 (−0.03)	0.30 (0.24)	0.15 (0.40)
	N	—CH_3	—NH_2
HemK (MAAM)			
R	−0.36	0.29	−0.06
TS	−0.39	0.40	0.00
P	−0.36	0.31	0.15

[a]ONIOM values in parentheses.

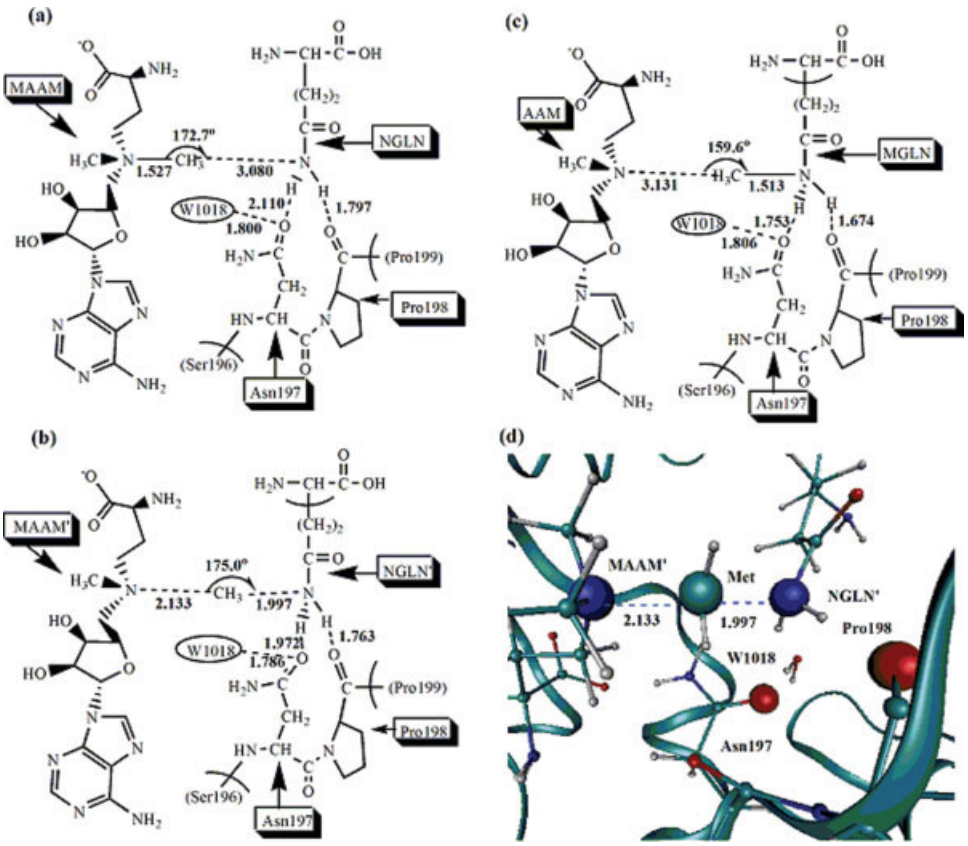

Figure 5. QM/MM-optimized structures of reactant (a), transition state (b and d), and product (c) in the methyl transfer reaction of the coenzyme-modified HemK (QM = B3LYP; MM = CHARMM; "W" indicates water). [Color figure can be viewed in the online issue, which is available at www.interscience.wiley.com.]

Conclusions

The methyl-transfer reactions catalyzed by HemK and the coenzyme-modified HemK have been studied by QM/MM methodologies. The calculations show that the methyl-transfer step can be characterized as a typical in-line S_N2 reaction. The QM/MM predicted barrier and the exthermicity for the methyl transfer catalyzed by HemK are 15.7 and 12.0 kcal/mol, respectively. The substantial barrier and instability of the product intermediate for the coenzyme-modified HemK warrants the nitrogen analogue of the SAM coenzyme for an inhibitor in the catalytic methyl-transfer reaction by HemK. MD simulation and QM/MM calculations show that the residues Asn197 and Pro198 in the active site are crucial in regulating the positioning of reactive groups and in reducing the activation energy. A comparison of different QM/MM calculations has confirmed the remarkable role of protein environments and solvent molecules in the enzymatic catalytic methyl-transfer reaction.

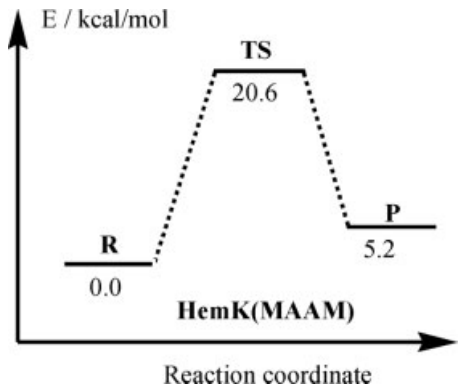

Figure 6. The QM-MM relative energy profiles along the methyl-transfer reaction pathway in the coenzyme-modified HemK (QM = B3LYP; MM = CHARMM).

Acknowledgments

We thank Professor Walter Thiel and Dr. Dongqi Wang at the Max-Planck-Institut für Kohlenforschung for support in using the ChemShell package.

References

1. Birda, P.; Wolffe, A. P. Cell 1999, 99, 451.
2. Ezhkova, F.; Tansey, W. P. Mol Cell 2004, 13, 435.

3. Falnes, P. O.; Johansen, P. F.; Seeberg, E. Nature 2002, 419, 178.
4. Aas, P. A.; Otterlei, M.; Falnes, P. O.; Vaagboe, C. B.; Skorpen, F.; Akbari, M.; Sundheim, O.; Bjoras, M.; Slupphaug, G.; Seeberg, E.; Krokan, H. E. Nature 2003, 421, 859.
5. Najbauer, J.; Orpiszewski, J.; Aswad, D. W. Biochemistry 1996, 35, 5183.
6. Strahl, B. D.; Allis, C. D. Nature 2000, 403, 41.
7. Clarke, S. Proc Natl Acad Sci USA 2002, 99, 1104.
8. Heurgué-Hamard, V.; Champ, S.; Engström, A.; Ehrenberg, M.; Buckingham, R. H. EMBO J 2002, 21, 769.
9. Nakahigashi, K.; Kubo, N.; Narita, S.; Shimaoka, T.; Goto, S.; Oshima, T.; Mori, H.; Maeda, M.; Wada, C.; Inokuchi, H. Proc Natl Acad Sci USA 2002, 99, 1473.
10. Schubert, H. L.; Phillips, J. D.; Hill, C. P. Biochemistry 2003, 42, 5592.
11. Nakayashiki, T.; Nishimura, K.; Inokuchi, H. Gene 1995, 153, 67.
12. Bujnicki, J. M.; Radlinska, M. IUBMB Life 1999, 48, 247.
13. Yang, Z.; Shipman, L.; Zhang, M.; Anton, B. P.; Roberts, R. J.; Cheng, X. J Mol Biol 2004, 340, 695.
14. (a) Gao, J.; Truhlar, D. G. Annu Rev Phys Chem 2002, 53, 467; (b) Gao, J.; Ma, S.; Major, D. T.; Nam, K.; Pu, J.; Truhlar, D. G. Chem Rev 2006, 106, 3188.
15. (a) Cui, Q.; Karplus, M. Adv Protein Chem 2003, 66, 315; (b) Field, M. J.; Bash, P. A.; Karplus, M. J Comput Chem 1990, 11, 700.
16. Zhang, Y.; Liu, H.; Yang, W. In Methods for Macromolecular Modeling; Schlick, T.; Gan, H. H., Eds.; Springer-Verlag: New York, 2002; pp. 332–354.
17. Warshel, A.; Levitt, M. J Mol Biol 1976, 103, 227.
18. Maseras, F.; Morokuma, K. J Comput Chem 1995, 16, 1170.
19. Kuhn, B.; Kollman, P. A. J Am Chem Soc 2000, 122, 2586.
20. Roca, M.; Andres, J.; Moliner, V.; Tunon, I.; Bertran, J. J Am Chem Soc 2005, 127, 10648.
21. Rod, T. H.; Rydberg, P.; Ryde, U. J Chem Phys 2006, 124, 174503.
22. Ruiz-Pernia, J. J.; Silla, E.; Tunon, I.; Marti, S. J Phys Chem B 2006, 110, 17663.
23. Hu, P.; Zhang, Y. K. J Am Chem Soc 2006, 128, 1272.
24. Soriano, A.; Castillo, R.; Christov, C. Andrès, J.; Moliner, V. Biochemistry 2006, 45, 14917.
25. Thompson, M. J.; Mekhalfia, A.; Hornby, D. P.; Blackburn, G. M. J Org Chem 1999, 64, 7467.
26. Thompson, M. J.; Mekhalfia, A.; Jakeman, D. L.; Phillips, S. E. V.; Phillips, K.; Porter, J.; Blackburn, G. M. J Chem Soc Chem Commun 1996, 791.
27. Brooks, B. R.; Bruccoleri, R. E.; Olafson, B. D.; States, D. J.; Swaminathan, S.; Karplus, M. J Comput Chem 1983, 4, 187.
28. (a) Lee, C.; Yang, W.; Parr, R. G. Phys Rev B 1988, 37, 785; (b) Becke, A. D. Phys Rev A 1988, 38, 3098; (c) Becke, A. D. J Chem Phys 1992, 96, 2155; (d) Becke, A. D. J Chem Phys 1992, 97, 9173; (e) Becke, A. D. J Chem Phys 1993, 98, 5648.
29. Frisch, M. J.; Trucks, G. W.; Schlegel, H. B.; Scuseria, G. E.; Robb, M. A.; Cheeseman, J. R.; Montgomery, J. A., Jr.; Vreven, T.; Kudin, K. N.; Burant, J. C.; Millam, J. M.; Iyengar, S. S.; Tomasi, J.; Barone, V.; Mennucci, B.; Cossi, M.; Scalmani, G.; Rega, N.; Petersson, G. A.; Nakatsuji, H.; Hada, M.; Ehara, M.; Toyota, K.; Fukuda, R.; Hasegawa, J.; Ishida, M.; Nakajima, T.; Honda, Y.; Kitao, O.; Nakai, H.; Klene, M.; Li, X.; Knox, J. E.; Hratchian, H. P.; Cross, J. B.; Bakken, V.; Adamo, C.; Jaramillo, J.; Gomperts, R.; Stratmann, R. E.; Yazyev, O.; Austin, A. J.; Cammi, R.; Pomelli, C.; Ochterski, J. W.; Ayala, P. Y.; Morokuma, K.; Voth, G. A.; Salvador, P.; Dannenberg, J. J.; Zakrzewski, V. G.; Dapprich, S.; Daniels, A. D.; Strain, M. C.; Farkas, O.; Malick, D. K.; Rabuck, A. D.; Raghavachari, K.; Foresman, J. B.; Ortiz, J. V.; Cui, Q.; Baboul, A. G.; Clifford, S.; Cioslowski, J.; Stefanov, B. B.; Liu, G.; Liashenko, A.; Piskorz, P.; Komaromi, I.; Martin, R. L.; Fox, D. J.; Keith, T.; Al-Laham, M. A.; Peng, C. Y.; Nanayakkara, A.; Challacombe, M.; Gill, P. M. W.; Johnson, B.; Chen, W.; Wong, M. W.; Gonzalez, C.; Pople, J. A.; Gaussian Inc. Wallingford CT, 2004.
30. MacKerell, A. D., Jr.; Bashford, D.; Bellott, M.; Dunbrack, R. L., Jr.; Evanseck, J. D.; Field, M. J.; Fischer, S.; Gao, J.; Guo, H.; Ha, S.; Joseph-McCarthy, D.; Kuchnir, L.; Kuczera, K.; Lau, F. T. K.; Mattos, C.; Michnick, S.; Ngo, T.; Nguyen, D. T.; Prodhom, B.; Reiher, W. E., III; Roux, B.; Schlenkrich, M.; Smith, J. C.; Stote, R.; Straub, J.; Watanabe, M.; Wiorkiewicz-Kuczera, J.; Yin, D.; Karplus, M. J Phys Chem B 1998, 102, 3586.
31. (a) Bakowies, D.; Thiel, W. J Phys Chem 1996, 100, 10580; (b) de Vries, A. H.; Sherwood, P.; Collins, S. J.; Rigby, A. M.; Rigutto, M.; Kramer, G. J. J Phys Chem B 1999, 103, 6133; (c) Sherwood, P.; de Vries, A. H.; Collins, S. J.; Greatbanks, S. P.; Burton, N. A.; Vincent, M. A.; Hillier, I. H. Faraday Discuss 1997, 106, 79.
32. Sherwood, P.; de Vries, A. H.; Guest, M. F.; Schreckenbach, G.; Catlow, C. R. A.; French, S. A.; Sokol, A. A.; Bromley, S. T.; Thiel, W.; Turner, A. J.; Billeter, S.; Terstegen, F.; Thiel, S.; Kendrick, J.; Rogers, S. C.; Casci, J.; Watson, M.; King, F.; Karlsen, E.; Sjovoll, M.; Fahmi, A.; Schäfer, A.; Lennartz, C. J Mol Struct (THEOCHEM) 2003, 632, 1.
33. Ahlrichs, R.; Bär, M.; Häser, M.; Horn, H.; Kölmel, C. Chem Phys Lett 1989, 162, 165.
34. Smith, W.; Forester, T. J Mol Graph 1996, 14, 136.
35. Billeter, S. R.; Turner, A. J.; Thiel, W. Phys Chem Chem Phys 2000, 2, 2177.
36. Cho, Y. K.; Northrop, D. B. Biochemistry 1999, 38, 7470.